Downloaded from on November 20, 2024 - Published by Cold Spring Harbor Laboratory Press

Dual degradation signals control Gli protein stability and tumor formation

Erik G. Huntzicker,[1,3] Ivette S. Estay,[1,3] Hanson Zhen,[1] Ludmila A. Lokteva,[1] Peter K. Jackson,[2,3] and Anthony E. Oro[1,3,4]

[1]Program in Epithelial Biology, [2]Department of Pathology, School of Medicine, and [3]Cancer Biology Graduate Program, Stanford University, Stanford, California 94305, USA

Regulated protein destruction controls many key cellular processes with aberrant regulation increasingly found during carcinogenesis. Gli proteins mediate the transcriptional effects of the Sonic hedgehog pathway, which is implicated in up to 25% of human tumors. Here we show that Gli is rapidly destroyed by the proteasome and that mouse basal cell carcinoma induction correlates with Gli protein accumulation. We identify two independent destruction signals in Gli1, D_N and D_C, and show that removal of these signals stabilizes Gli1 protein and rapidly accelerates tumor formation in transgenic animals. These data argue that control of Gli protein accumulation underlies tumorigenesis and suggest a new avenue for antitumor therapy.

Supplemental material is available at http://www.genesdev.org.

Received October 3, 2005; revised version accepted December 1, 2005.

Factors controlling protein destruction are critical for the timing of key processes such as the cell cycle, apoptosis, and cell fate decisions, with aberrant regulation increasingly found during carcinogenesis (Pickart 2004; Yamasaki and Pagano 2004). Inappropriate Sonic hedgehog (Shh) signaling results in a panoply of birth defects and is implicated in up to 25% of human tumors (Callahan and Oro 2001; Lum and Beachy 2004). While the Gli family of proteins mediates the transcriptional effects of Shh (Methot and Basler 2001; Ruiz i Altaba et al. 2002), the mechanism by which Gli proteins are regulated to achieve changes in pathway output remains poorly understood. Studies in mice and humans show that Shh target gene induction is sufficient to induce a variety of tumors including basal cell carcinomas (BCCs) (Oro et al. 1997; Nilsson et al. 2000; Hutchin et al. 2005). However, there is a wide variability in the onset and severity of phenotypes among patients with mutations in the Shh pathway (Wicking et al. 1997), and a noticeably wide variability of tumor onset in animal models (Oro and Higgins 2003; Hutchin et al. 2005). This suggests the possibility that additional, previously uncharacterized, cellular processes regulate pathway output. Here we show that Gli protein accumulation correlates with tumor formation and stabilizing mutations in Gli protein dramatically accelerate tumor induction.

Results and Discussion

While expression of either Gli1 or Gli2 in the epidermis of transgenic mice induces BCCs (Fig. 1a), we have observed a considerable delay in the appearance of Gli-dependent tumors. Analysis of transgenic mice expressing Gli2 revealed an average latency of 7 mo before tumor appearance (Fig. 1b). We ruled out changes in transcription of the transgene with age as a cause of the tumors, as similar levels of RNA are seen in both age groups as measured by quantitative PCR (Fig. 1c). This suggested the existence in keratinocytes of additional processes, whose loss or dysregulation is required to permit Gli activity and direct tumor formation. Our previous studies indicated that differential accumulation of Gli protein plays an important role in restricting Shh target gene induction in interfollicular epithelium (Oro and Higgins 2003). Indeed, we detected no transgenic Gli protein in normal skin, whereas we found high levels in the BCC tumors (Fig. 1d). Cultured explants of primary keratinocytes from normal skin also contained little detectable Gli protein (Fig. 1e). However, treatment of these cells with the proteasome inhibitor MG132 caused full-length Gli2 protein to accumulate many fold within 3 h, confirming the presence of an active Gli2 protein destruction mechanism. These data support the conclusion that proteasome-dependent Gli protein destruction underlies the latency in Shh target gene response.

To study the molecular mechanisms that govern Gli protein degradation, we chose to focus our initial studies on Gli1, which, unlike Gli2 or Gli3, is primarily a transcriptional activator and is not processed to a repressor form (Dai et al. 1999; von Mering and Basler 1999). In this way, Gli protein function and degradation could be examined independently of proteolytic processing and transcriptional repressor regulation. We tested Gli1 stability in a variety of in vitro settings and found that Gli1 is degraded by the proteasome. In *Xenopus* egg extracts, a system where the ubiquitin–proteasome system (UPS) is known to be active to control β-catenin and IκB stability (Winston et al. 1999; Margottin-Goguet et al. 2003), ^{35}S-labeled Gli1 protein is destroyed in a proteasome-dependent manner, with a half-life of 40 min (Fig. 1f). Similar kinetics are seen in a variety of cultured normal and cancer cells, including the Shh-responsive NIH 3T3 cells (Fig. 1g; Taipale et al. 2000). We ruled out degradation of Gli1 by other mechanisms such as lysosomal degradation (Dai et al. 2003), as cathepsin and lysosome inhibitors (E64 and chloroquine, respectively) had no effect on Gli levels (Fig. 1h). The efficacy of these inhibitors was confirmed in primary human keratinocytes where they inhibit the EGF-dependent lysosomal destruction of EGFR (Fig. 1h). These data provide strong support for destruction of vertebrate Gli1 by the UPS.

To identify signals that allow Gli1 to interact with the UPS, we were guided by the previous finding in *Drosophila* that the βTrCP locus is required for Ci processing (Jiang and Struhl 1998). The degron DSGXXS, recognized by βTrCP, is present in vertebrate regulatory pro-

[*Keywords*: Hedgehog; Gli; β-TRCP; proteasome; basal cell carcinoma; hair follicle]
[4]**Corresponding author.**
E-MAIL oro@cmgm.stanford.edu; FAX (650) 723-8762.
Article published online ahead of print. Article and publication date are at http://www.genesdev.org/cgi/doi/10.1101/gad.1380906.

Downloaded from on November 20, 2024 - Published by Cold Spring Harbor Laboratory Press

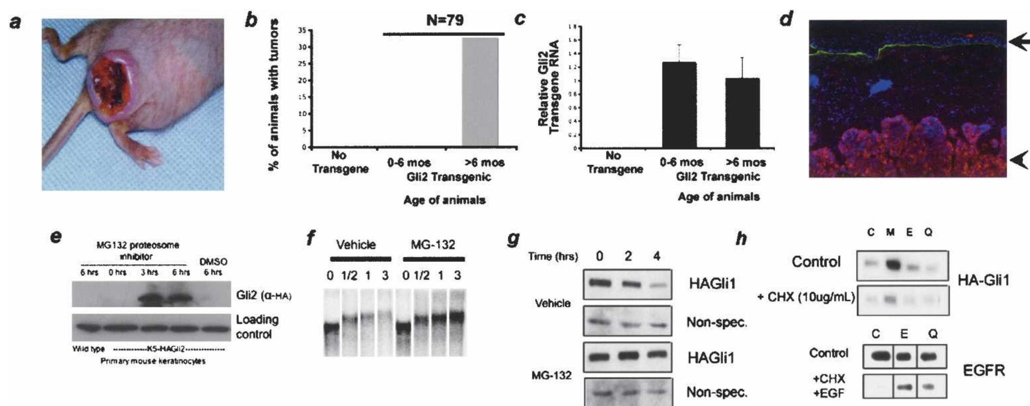

Figure 1. Onset of BCC formation correlates with Gli protein accumulation. (*a*) Clinical appearance of focal BCCs induced in transgenic animals expressing Gli2 in the skin epithelium with the keratin 5 promoter. (*b*) Bar graph showing representative onset of tumors in K5-Gli2 mice. (*c*) Quantitative PCR of Gli2 RNA levels from skin of wild-type or Gli2 transgenic animals of indicated age. Gli2 RNA levels in each sample were normalized to those of GAPDH. Error bars are standard error of the mean (SEM). (*d*) Immunofluorescence with anti-HA (red) antibody showing protein accumulation only in BCC tumor (arrowhead), not in interfollicular epidermis (arrow). (Green) Anti-laminin 5; (blue) Hoechst. (*e*) Western blot of lysates from explanted K5-Gli2 keratinocytes demonstrating the rapid accumulation of Gli2 protein with the addition of the proteasome inhibitor MG132, but not with DMSO. (*f*) Autoradiogram of ^{35}S-labeled Gli1 mixed with *Xenopus* oocyte extract. Gli1 is degraded in a proteasome-dependent manner with a half-life of ~40 min. (*g*) Western blot of HA-Gli1 in NIH 3T3 cells showing rapid, proteasome-dependent destruction. The nonspecific band demonstrates equal protein loading. (*h*) HA-Gli1 protein is rapidly degraded (C) via a process inhibited by proteasome inhibitors (M), but not cathepsin or lysosomal inhibitors E64 (E) or chloroquine (Q), respectively. The efficacy of the E64 and chloroquine used in this experiment was confirmed by their ability to inhibit ligand-dependent lysosomal destruction of EGFR in primary human keratinocytes.

teins β-catenin, IκBα/β, and Emi1 (Spencer et al. 1999), although it is absent from Ci. In spite of this, we have identified a C-terminal motif, DSGVEM, that is conserved in chordate Gli homologs and vertebrate Gli1 and Gli2 proteins (Fig. 2a). To determine if the DSGVEM motif of human Gli1 mediates association with βTrCP1, reciprocal immunoprecipitations were performed from NIH 3T3 cells transfected with myc-tagged βTrCP1 and HA-tagged Gli1 (Fig. 2b). Gli1 protein lacking the DSGVEM motif (Gli1ΔD_C) failed to associate with βTrCP and exhibited delayed degradation kinetics (Fig. 2c). Levels of βTrCP appeared to be limiting for Gli1 degradation, as increasing the levels of βTrCP protein significantly decreased steady-state levels of Gli1 protein (Fig. 2d). Consistent with its role as an E3 ligase, βTrCP association with Gli1 facilitated ubiquitination. In ubiquitin coimmunoprecipitation assays, ubiquitinylated Gli1 (ΔN398), but not Gli1ΔD_C (ΔN398), could be detected in the presence of overexpressed βTrCP1 (Fig. 2e). Previous studies have shown that Protein kinase A (PKA) can enhance βTrCP-dependent Ci cleavage in *Drosophila* (Wang et al. 1999; Jia et al. 2004). We saw similar effects on Gli1, as inhibition of PKA impeded destruction (Supplementary Fig. 2a), and Gli1 constructs lacking consensus PKA sites in the C terminus failed to bind βTrCP and exhibited delayed destruction kinetics (Supplementary Fig. 2a,b). These data demonstrate that degron D_C mediates Gli destruction via the βTrCP–ubiquitin ligase complex.

While βTrCP-dependent degradation clearly plays a role in Gli1 destruction, the Gli1ΔD_C mutation only partially altered the destruction kinetics of Gli1 protein in cultured cells. At 3 h after cycloheximide addition, destruction of Gli1ΔD_C was decreased by only ~25% relative to wild-type Gli1 (47.1% ± 6% vs. 21% ± 5%, Avg. ± SEM) (Fig. 3b). This argued that additional signals control Gli1 degradation. Through focused mutagenesis, we found that a small deletion of the N terminus further stabilized Gli1. As with the D_C degron, degron D_N mutations (GliΔN1–116, referred to as Gli1ΔD_N) alone had modest effects on Gli destruction kinetics in vitro (3 h: 40.1% ± 6% vs. 21% ± 5%, Avg. ± SEM) (Fig. 3b). However, Gli1 lacking both degrons (double mutant; Gli1ΔD_NΔD_C became stable, possessing destruction kinetics similar to that with addition of proteasome inhibitor (Figs. 3b, 1g). This argued for an additional degron in the N terminus. Further mutagenesis narrowed the region containing the degradation signal to residues 51–116 (Supplementary Fig. 3). This region contains a stretch of highly conserved residues present in all vertebrate Gli genes and in *Drosophila* Ci (Fig. 3a), suggesting that the destruction signal may be found in many Gli proteins.

We next determined whether degron D_N functioned independently of degron D_C. We tested whether βTrCP binding depends on D_N. Consistent with the notion of distinct signals, coimmunoprecipitation studies showed that βTrCP bound equally well to both wild-type Gli1 and the Gli1ΔD_N mutant (Fig. 3c). Moreover, we tested whether degron D_N could confer instability to a heterologous protein. Green Fluorescent Protein (GFP) is a stable protein with a long half-life. Addition of amino acids 1–208, a region that encompasses degron D_N sequences, destabilized GFP in a proteasome-dependent fashion, giving it a half-life of 180 min (Fig. 3d). Together, these data suggest the two destruction signals function independently.

Degron D_N is immediately adjacent to the binding site for Sufu (Fig. 3a), a powerful negative regulator of the Shh pathway, suggesting that the degron might work in conjunction with Sufu. Consequently, we tested whether D_N mutations affected the known Sufu functions of transcriptional corepression and Gli sequestration in the cytosol (Ding et al. 1999; Kogerman et al. 1999; Cheng and Bishop 2002). Gli1ΔD_N bound to Sufu as well as wild-type Gli1 in GST pull-down (Fig. 3e) assays. Also, Gli1

Downloaded from on November 20, 2024 - Published by Cold Spring Harbor Laboratory Press

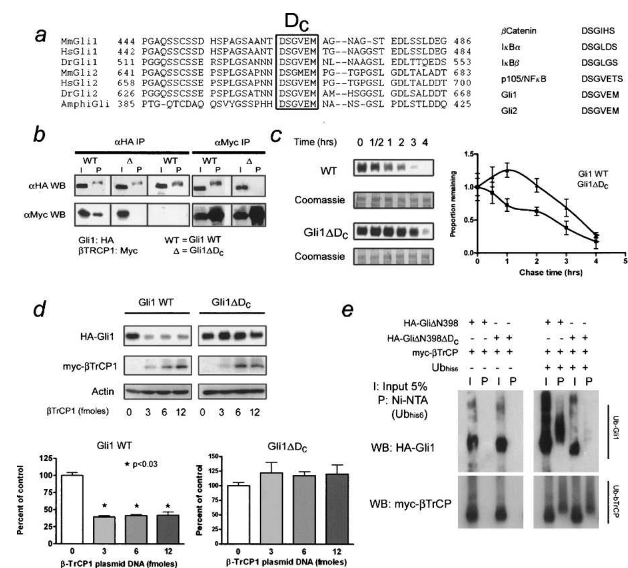

Figure 2. Degron D_C (DSGVEM) mediates Gli1 destruction via the βTrCP destruction complex. (*a*, *left*) Alignment of chordate Gli sequences showing conserved D_C sequence. The box details key residues that bind βTrCP. (*Right*) βTrCP-binding sequences from other vertebrate proteins. (*b*) Reciprocal coimmunoprecipitation of HA-Gli1 or HA-Gli1ΔD_C with myc-βTrCP. Note the lack of βTrCP binding in the mutant. The characteristic mobility shift of immunoprecipitated Gli1 is not an artifact of βTrCP overexpression as this shift is observed even in its absence. (*c*) Degradation of transfected Gli1 in NIH 3T3 cells. Note the small but significant delay in destruction kinetics of the mutant versus wild-type protein. The densitometry of both assays is shown to the *right* and is representative of three independent experiments. Equal sample loading and transfer was confirmed by post-staining of the experimental membranes with Coomassie blue. The 150–250-kDa region of the membranes is shown. (*d*) Western blot of Gli1 or Gli1ΔD_C and increasing amounts of transfected βTrCP. Note the decreased steady-state levels of wild-type, but not mutant Gli1. The difference is quantified *below* and is representative of three independent experiments. Error bars are standard error of the mean (SEM). (*e*) Coimmunoprecipitation assay of 6X-His-tagged ubiquitin and HA-Gli1ΔN398 containing degron D_C or HA-Gli1ΔN398ΔD_C mutant. Ubiquitinylated Gli (*top* panel) is detected in the wild-type Gli1 C terminus, but not the ΔD_C mutant, in the presence of βTrCP (*bottom* panel).

mutants had a similar subcellular distribution to wild-type Gli1 and accumulated in the nucleus with equal efficiency in the presence of leptomycin (Fig. 3f). These data argue that the N-terminal degron regulates Gli1 stability via a unique Sufu- and degron D_C-independent pathway.

Gli1 is known to activate transcription of Shh target genes via a transactivation domain in its C terminus (Yoon et al. 1998). To determine the functional significance of stabilizing Gli, we assessed the transcriptional activity of the mutants on Gli-responsive promoters (Taipale et al. 2000). Gli1ΔD_C and Gli1ΔD_N displayed modest increases in transcription when the same molar amount of plasmid was transfected into cells, with the double mutant displaying threefold higher target gene induction compared with wild-type Gli1 (Fig. 3g,h). This increase could be due to increased transactivation ability or increased protein levels. Analysis of protein levels relative to transcriptional output demonstrated a clear linear relationship between the amount of Gli1 protein for each of the mutants and reporter gene output (Fig. 3g,h). These data argue that the greater transcriptional activity of the mutants is due to increased protein stability rather than transactivation ability.

Tumor induction in Gli transgenic animals correlates with Gli protein accumulation. If the degrons identified in our studies are responsible for restricting Gli1 protein accumulation in vivo, then expressing Gli1 without these signals should shorten the latency to tumor induction. We assayed skin phenotypes of several lines of transgenic animals expressing different mutants of Gli1 in the basal layer of stratified epithelia. As expected, transgenic animals expressing wild-type Gli1 were born normally with no detectable transgenic Gli protein (Fig. 4b,l), and developed the predicted tumor phenotype at 6–8 wk after birth (Oro and Higgins 2003; data not shown). In contrast, animals expressing double-mutant Gli1 (Gli$\Delta D_N \Delta D_C$) exhibited Gli protein accumulation at the time of birth in tumor and nontumor epithelium (Fig. 4c; Supplementary Fig. 4). The Gli$\Delta D_N \Delta D_C$-expressing animals died at birth with shallow skin ulcers clinically similar to BCCs throughout the body. The tumors demonstrated characteristic features of BCCs (Fig. 4c,m; Supplementary Fig. 4; Oro et al. 1997; Callahan et al. 2004), including the up-regulation of *ptch1* (Fig. 4r). Moreover, the tumors were rapidly dividing as evidenced by the significant increase in Ki67 staining and displayed the BCC marker keratin 17 (Supplementary Fig. 4). This demonstrates that altered protein accumulation can directly accelerate tumor induction.

In cultured cells, both degrons were highly active in restricting Gli1 levels. However, depending on the specificity and/or capacity of the operative degradation pathway, one of the degrons may play a more active role in a given in vivo context. We determined the relative contribution of each degron to Gli1 destruction by comparing the phenotype of single Gli mutant transgenic mice to those expressing Gli$\Delta D_N \Delta D_C$. In the skin, Gli1 mutants lacking degron D_C displayed a much stronger phenotype than those lacking degron D_N (Fig. 4v). While both GliΔD_C and GliΔD_N transgenic mice were viable and lacked the ulcerating lesions seen in the double mutant, GliΔD_C mutants demonstrated BCC-like lesions at birth more comparable to those expressing Gli$\Delta D_N \Delta D_C$ (depth of invasion, 111 µM vs. 140 µM, respectively) (Fig. 4d). GliΔD_N transgenic animals had small BCC-like proliferations that developed slightly after birth and appeared to come directly off the hair follicle (Fig. 4e). Also, many GliΔD_N mutant lesions were benign hair follicle tumors, indicative of lower Shh target gene induction (Callahan and Oro 2001; Grachtchouk et al. 2003). In each of the Gli mutants, the distribution of Gli protein was both nuclear and cytoplasmic, providing further evidence that the degron sequences do not play a role in nucleocytoplasmic shuttling of Gli1 (Fig. 4l–p). The phenotypic differences within each group could not be attributed to transgene expression differences, as only steady-state protein levels by IHC, not transgene copy number or RNA expression level, correlated with the phenotype (Fig. 4; Supplementary Fig. 5). These data demonstrate the combinatorial action of both D_C and D_N degrons in preventing ectopic Shh target gene induction and provide in vivo support for the role of Gli destruction in controlling tumor formation.

Here we have shown that Gli1 protein contains two destruction signals that regulate protein stability and tu-

Downloaded from on November 20, 2024 - Published by Cold Spring Harbor Laboratory Press

mor formation (Supplementary Fig. 1). As with other key regulatory proteins such as myc, p53, IκB, and β-catenin, there appears to be a finely balanced control of Gli1 protein levels to allow for proper target gene induction while preventing epithelial tumor formation. Our data suggest that the BCC tumors observed in the K5Gli2 transgenic mice likely arise as a result of secondary changes that lead to Gli2 stabilization rather than as a result of gradual saturation of the destruction machinery. Arguing against saturation is the lack of increased protein in adjacent normal tissue or in the explanted cells from older animals. Furthermore, with the addition of proteasome inhibitors, we see rapid accumulation of Gli2 protein. This suggests that halting the destruction of Gli proteins is an early step in the tumor process and that cellular changes that allow Gli1 protein accumulation may contribute to human carcinogenesis (Kinzler et al. 1988). Similarly, targeted therapies that delay the onset of Gli accumulation may have potent antitumor properties.

Our study illustrates how two destruction signals cooperate to prevent Gli protein accumulation, target gene induction, and subsequent tumor formation. While a role for βTrCP has been implicated in Ci processing, the present study is the first to demonstrate that it acts by directly binding Gli to facilitate ubiquitinylation and destruction. Interestingly, while Ci and Gli1 are both directed by PKA and βTrCP to interact with the proteasome, the end result differs in that Gli1 is degraded but not cleaved. This could be due to either the particular amino acid sequence of the degron or to surrounding amino acids that influence βTrCP/UPS function. The identified Gli degron differs significantly from that of β-catenin, Emi1, and IkB in that it lacks a second serine shown to be important for sequential phosphorylation and contains a phosphomimetic glutamic acid residue (Amit et al. 2002; Moshe et al. 2004). Future studies will focus on whether these sequence differences are sufficient to account for the different final disposition of the protein. This study further identifies a novel degron, D_N, that shares little identity with other known degradation signals. The conserved sequences in this degron are found in both Gli2 and Gli3, and removal of the region containing them has been associated with activation of Gli2 (Sasaki et al. 1999; Mill et al. 2003). Our data suggest that a portion of this activation may be due to Gli2 protein stabilization via degron D_N rather than simply loss of transcriptional repressor activity.

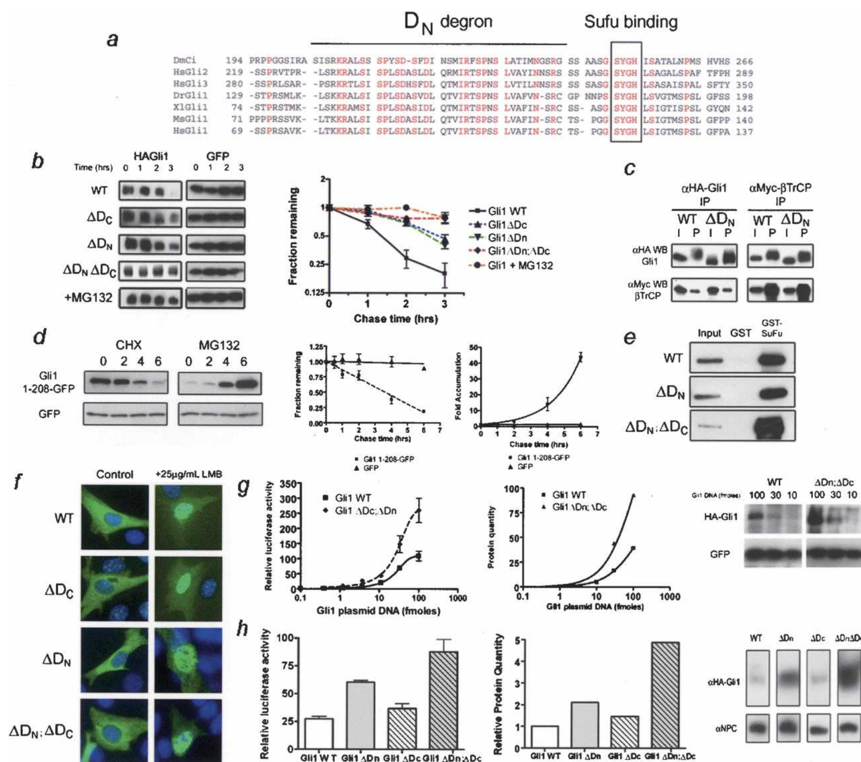

Figure 3. Degron D_N mediates Gli destruction independent of D_C or Sufu function. (*a*) Alignment showing the conserved N-terminal region containing degron D_N. A solid line indicates the most highly conserved region that is deleted in the D_N mutant, while the boxed area shows the Sufu-binding site, which is retained in the D_N mutant. (*b*) Destruction assays of HA-Gli1 in NIH 3T3 cells showing the effects of single D_C, D_N, and double mutants in comparison to wild-type (WT) Gli1 in the presence and absence of MG132. The densitometery of blots is shown to the *right* and is based on three independent experiments. Note that results are plotted on the base 2 logarithmic scale. Error bars are standard error of the mean (SEM). (*c*) Coimmunoprecipitation of wild-type and mutant Gli with βTrCP. Note that the D_N mutation does not affect the binding of βTrCP to degron D_C. (*d*) Changes in levels of green fluorescent protein (EGFP) fused to Gli1 N-terminal residues (*top*), or EGFP (*bottom*), in the presence of cycloheximide (*left*) or MG132 (*right*). The amount of fusion protein is identical at $t = 0$, but the exposure time for the *left* and *right* panels differs to avoid signal saturation. The densitometry is shown to the *right* with results plotted on a linear scale. The results are representative of three independent experiments. Error bars are SEM. (*e*) Coprecipitation assays with GST-Sufu and lysates from cells containing wild-type or mutant Gli proteins. Note that the Gli1ΔD_N mutation leaves Sufu binding intact. (*f*) Immunofluorescence of Gli1 shows similar subcellular localization of wild-type and mutant Gli1 proteins in the absence (*left*) or presence (*right*) of the Crm1-inhibitor leptomycin B. (*g*, *left*) Luciferase transcription assays of wild-type and double-mutant Gli1 protein with increasing amounts of transfected moles of plasmid. Error bars are SEM. Densitometry (*middle*) of Western blots (*right*) showing the amount of steady-state protein accumulation corresponding to the increase in luciferase activity. (*h*, *left*) Luciferase transcription assays of wild-type, single, and double-mutant Gli1 proteins. Error bars are SEM. Western blot (*right*) of levels of Gli1 protein in luciferase assay and quantitation (*middle*) of protein levels normalized for loading and transfer efficiency determined by immunoblot for nuclear pore complex (NPC).

Material and methods

Destruction assays

***Xenopus* egg extracts.** *Xenopus* egg cytoplasmic extracts were prepared fresh as previously described (Reimann et al. 2001). Substrate proteins were in vitro translated in the presence of ^{35}S-methionine using the TnT IVT system (Promega). IVT protein was added to egg extract to 10% of final volume. Destruction assays were conducted in a final volume of 2–10 µL, and stopped by addition of 2× Sample buffer and snap-freezing in liquid nitrogen. In some experiments, MG-132 (Calbiochem) was added to a final concentration of 1 mM.

NIH 3T3. NIH 3T3 cells were transfected as described above. Two days after transfection cycloheximide was added to final concentration of 20 µg/mL and samples were harvested in 2× Sample buffer at various time points. Alternatively, cycloheximide was added at various time points

Downloaded from on November 20, 2024 - Published by Cold Spring Harbor Laboratory Press

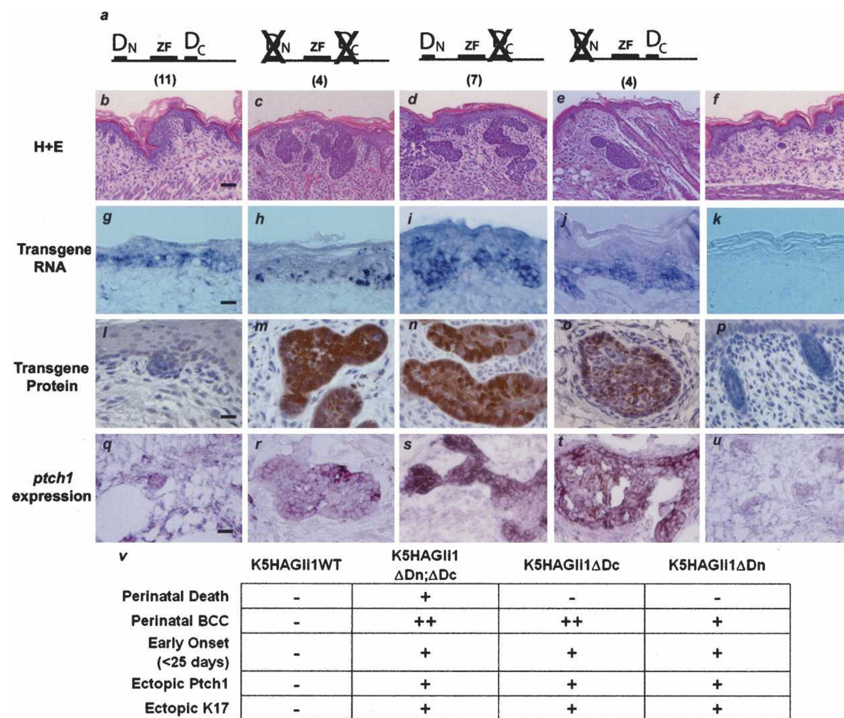

	K5HAGli1WT	K5HAGli1 ΔDn;ΔDc	K5HAGli1ΔDc	K5HAGli1ΔDn
Perinatal Death	-	+	-	-
Perinatal BCC	-	++	++	+
Early Onset (<25 days)	-	+	+	+
Ectopic Ptch1	-	+	+	+
Ectopic K17	-	+	+	+

Figure 4. Removal of two destruction signals rapidly accelerates tumor induction. (*a*) Diagram of Gli1 wild-type (*b*,*g*,*l*,*q*), Gli1$\Delta D_C \Delta D_N$ (*c*,*h*,*m*,*r*), Gli1ΔD_C (*d*,*i*,*n*,*s*), Gli1ΔD_N (*e*,*j*,*o*,*t*), or nontransgenic (*f*,*k*,*p*,*u*) mice analyzed in this study. The number of independent founders is shown in parentheses. (*b*–*f*) Representative H&E sections from each founder line. Note BCC-like lesions from interfollicular epithelium in *c* and *d*, and BCC-like tumors from hair follicle in *e*. Bar, 50 µm. (*g*–*k*) In situ hybridization of transgene expression using transgene-specific *gli1* probe. Bar, 25 µm. (*l*–*p*) Immunohistochemistry with anti-HA antibody for Gli1 protein. Note the absence of Gli1 protein in wild-type Gli1 transgenics and nuclear and cytoplasmic distribution in mutant Gli animals. Bar, 10 µm. (*q*–*u*) In situ hybridization with *ptch1* probe showing Shh target gene induction in tumors. Bar, 10 µm. (*v*) Table of representative features of each group of Gli1 transgenic mice.

prior to lysis of all samples in 2× Sample buffer. Both approaches yielded similar results. In some experiments MG-132 (Calbiochem) was added to a final concentration of 30 µM 1 h prior to destruction assay. HA-tagged Gli1 proteins were detected with a mouse-anti-HA monoclonal antibody (Covance). Equal transfection was confirmed by blotting with a mouse antibody for EGFP (Roche), and loading and transfer efficiency were confirmed by blotting with a mouse antibody to β-actin (Sigma).

Primary human keratinocytes. Primary human foreskin keratinocytes were passaged in Keratinocyte-SFM medium (Invitrogen) supplemented with bovine pituitary extract and recombinant human EGF (Invitrogen) and cultured in unsupplemented Keratinocyte-SFM for 24 h prior to the destruction assay. For destruction assay, recombinant human EGF (Invitrogen) was added to a final concentration of 100 ng/mL with cycloheximide to a concentration of 100 µg/mL. Chloroquine (12.5 g/mL; Sigma) or E64 (25 µM; Calbiochem) were added 1 h prior to beginning the destruction assay. Samples were harvested at various time points in 2× Sample buffer. EGFR protein was detected with a rabbit antibody to EGFR (Santa Cruz Biotechnology). Equal sample loading was confirmed by blotting for β-actin.

Mice

All mouse studies were performed in accordance with the policies of the Stanford IUPAC. K5Gli2 animals were generated using full-length mouse Gli2 (Sasaki et al. 1999) containing a triple HA tag on the N terminus in pENTR1A (Invitrogen) and then recombined into a transgenic vector containing the bovine keratin 5 promoter (Ramirez et al. 1994; Callahan et al. 2004) using Gateway cloning (Invitrogen). Five independent lines were generated that had similar phenotypes. Line #70 was expanded and quantified. K5Gli1 wild-type, K5Gli1ΔD_C; ΔD_N, K5Gli1ΔD_C, and K5Gli1ΔD_N were constructed as described in the Plasmid section in the Supplemental Material and then recombined into the bovine keratin 5 promoter by Gateway cloning. Transgene copy number was determined by quantitative real-time PCR (Brilliant Sybr Green; Stratagene) using DNA isolated from transgenic mouse tails. We used primers specific to the 3′-region of human Gli1 (F: GCCGTGCTAAAGCTCCAGTGAACAC; R: AGAAGTCGAGGTGGTGCTGCTGCCC). These primers did not amplify mouse Gli1. A 10-fold dilution series of transgene plasmid diluted into a constant amount of nontransgenic mouse DNA was used as a standard to determine transgene copy number in a given amount of tail DNA. Mouse GAPDH (GAPDH F: TCTTCTTGTGCAGTGCCAGCCTCGTCC; R: GACTGTGCCGTTGAATTTGCCGTGAGTG) and mouse Gli2 primers (F: CCTCCCTGGGAAGAAGACTTGCGTCTAC; R: TCAATGCCTTCAACCTTCCGCTCAAC) were used as controls for DNA loading and quality. Copy number results are expressed as copies per diploid genome. Expression analysis of transgene expression was performed by quantitative real-time RT–PCR (Brilliant Sybr Green; Stratagene) according to the manufacturer's instructions. RNA was isolated from right hind-limb tissue using Trizol reagent (Invitrogen). Mouse Keratin 5 primers (F: CTCCAGGAACCATCATGTCTCGCCAGTC; R: CACCACCGAAGCCAAAGCCACTACCAG) were used to control for RNA loading and quality. Template quantity was determined using the delta–delta CT method according to the manufacturer's instructions.

Acknowledgments

We thank C.A. Callahan for help in making transgenic Gli2 animals; Lei Chen and the Stanford Transgenic Facility for help with pronuclear injections; and Paul Khavari, James Chen, Howard Chang, and the Oro laboratory for comments on the manuscript. This work is funded by NIH grants R01ARO46786 (to A.E.O) and R01GM60439 (to P.K.J), a Stanford Graduate Fellowship (to E.G.H.), and the Cancer Biology graduate program (to I.S.E.).

References

Amit, S., Hatzubai, A., Birman, Y., Andersen, J.S., Ben-Shushan, E., Mann, M., Ben-Neriah, Y., and Alkalay, I. 2002. Axin-mediated CKI phosphorylation of β-catenin at Ser 45: A molecular switch for the Wnt pathway. *Genes & Dev.* **16:** 1066–1076.

Callahan, C.A. and Oro, A.E. 2001. Monstrous attempts at adnexogenesis: Regulating hair follicle progenitors through Sonic hedgehog signaling. *Curr. Opin. Genet. Dev.* **11:** 541–546.

Callahan, C., Ofstad, T., Horng, L., Wang, J., Zhen, H., and Oro, A. 2004. MIM/BEG4, a Sonic hedgehog-responsive gene that potentiates Gli-dependent transcription. *Genes & Dev.* **18:** 2724–2729.

Cheng, S.Y. and Bishop, J.M. 2002. Suppressor of Fused represses Gli-mediated transcription by recruiting the SAP18–mSin3 corepressor complex. *Proc. Natl. Acad. Sci.* **99:** 5442–5447.

Dai, P., Akimaru, H., Tanaka, Y., Maekawa, T., Nakafuku, M., and Ishii, S. 1999. Sonic Hedgehog-induced activation of the Gli1 promoter is mediated by GLI3. *J. Biol. Chem.* **274:** 8143–8152.

Dai, P., Akimaru, H., and Ishii, S. 2003. A hedgehog-responsive region in the *Drosophila* wing disc is defined by debra-mediated ubiquitination and lysosomal degradation of Ci. *Dev. Cell* **4:** 917–928.

Ding, Q., Fukami, S., Meng, X., Nishizaki, Y., Zhang, X., Sasaki, H., Dlugosz, A., Nakafuku, M., and Hui, C. 1999. Mouse suppressor of fused is a negative regulator of Sonic hedgehog signaling and alters the subcellular distribution of Gli1. *Curr. Biol.* **9:** 1119–1122.

Grachtchouk, V., Grachtchouk, M., Lowe, L., Johnson, T., Wei, L., Wang,

Downloaded from on November 20, 2024 - Published by Cold Spring Harbor Laboratory Press

A., de Sauvage, F., and Dlugosz, A.A. 2003. The magnitude of Hedgehog signaling activity defines skin tumor phenotype. *EMBO J.* **22:** 2741–2751.

Hutchin, M.E., Kariapper, M.S., Grachtchouk, M., Wang, A., Wei, L., Cummings, D., Liu, J., Michael, L.E., Glick, A., and Dlugosz, A.A. 2005. Sustained Hedgehog signaling is required for basal cell carcinoma proliferation and survival: Conditional skin tumorigenesis recapitulates the hair growth cycle. *Genes & Dev.* **19:** 214–223.

Jia, J., Tong, C., Wang, B., Luo, L., and Jiang, J. 2004. Hedgehog signalling activity of Smoothened requires phosphorylation by protein kinase A and casein kinase I. *Nature* **432:** 1045–1050.

Jiang, J. and Struhl, G. 1998. Regulation of the Hedgehog and Wingless signalling pathways by the F-box/WD40-repeat protein Slimb. *Nature* **391:** 493–496.

Kinzler, K.W., Ruppert, J.M., Bigner, S.H., and Vogelstein, B. 1988. The GLI gene is a member of the Kruppel family of zinc finger proteins. *Nature* **332:** 371–374.

Kogerman, P., Grimm, T., Kogerman, L., Krause, D., Undén, A.B., Sandstedt, B., Toftgård, R., and Zaphiropoulos, P.G. 1999. Mammalian Suppressor-of-fused modulates nuclear-cytoplasmic shuttling of Gli-1. *Nat. Cell Biol.* **1:** 312–319.

Lum, L. and Beachy, P.A. 2004. The Hedgehog response network: Sensors, switches, and routers. *Science* **304:** 1755–1759.

Margottin-Goguet, F., Hsu, J.Y., Loktev, A., Hsieh, H.M., Reimann, J.D., and Jackson, P.K. 2003. Prophase destruction of Emi1 by the SCF(βTrCP/Slimb) ubiquitin ligase activates the anaphase promoting complex to allow progression beyond prometaphase. *Dev. Cell* **4:** 813–826.

Methot, N. and Basler, K. 2001. An absolute requirement for Cubitus interruptus in Hedgehog signaling. *Development* **128:** 733–742.

Mill, P., Mo, R., Fu, H., Grachtchouk, M., Kim, P.C., Dlugosz, A.A., and Hui, C.C. 2003. Sonic hedgehog-dependent activation of Gli2 is essential for embryonic hair follicle development. *Genes & Dev.* **17:** 282–294.

Moshe, Y., Boulaire, J., Pagano, M., and Hershko, A. 2004. Role of Polo-like kinase in the degradation of early mitotic inhibitor 1, a regulator of the anaphase promoting complex/cyclosome. *Proc. Natl. Acad. Sci.* **101:** 7937–7942.

Nilsson, M., Unden, A., Krause, D., Malmqwist, U., Raza, K., Zaphiropoulos, P., and Toftgard, R. 2000. Induction of basal cell carcinomas and trichoepitheliomas in mice overexpressing Gli-1. *Proc. Natl. Acad. Sci.* **97:** 3438–3443.

Oro, A.E. and Higgins, K.M. 2003. Hair cycle regulation of Hedgehog signal reception. *Dev. Biol.* **255:** 238–248.

Oro, A.E., Higgins, K.M., Hu, Z., Bonifas, J.M., Epstein Jr., E.H., and Scott, M.P. 1997. Basal cell carcinomas in mice overexpressing Sonic hedgehog. *Science* **276:** 817–821.

Pickart, C.M. 2004. Back to the future with ubiquitin. *Cell* **116:** 181–190.

Ramirez, A., Bravo, A., Jorcano, J.L., and Vidal, M. 1994. Sequences 5′ of the bovine keratin 5 gene direct tissue- and cell-type-specific expression of a lacZ gene in the adult and during development. *Differentiation* **58:** 53–64.

Reimann, J.D., Freed, E., Hsu, J.Y., Kramer, E.R., Peters, J.M., and Jackson, P.K. 2001. Emi1 is a mitotic regulator that interacts with Cdc20 and inhibits the anaphase promoting complex. *Cell* **105:** 645–655.

Ruiz i Altaba, A., Sanchez, P., and Dahmane, N. 2002. Gli and Hedgehog in cancer: Tumours, embryos and stem cells. *Nat. Rev. Cancer* **2:** 361–372.

Sasaki, H., Nishizaki, Y., Hui, C., Nakafuku, M., and Kondoh, H. 1999. Regulation of Gli2 and Gli3 activities by an amino-terminal repression domain: Implication of Gli2 and Gli3 as primary mediators of Shh signaling. *Development* **126:** 3915–3924.

Spencer, E., Jiang, J., and Chen, Z.J. 1999. Signal-induced ubiquitination of IκBα by the F-box protein Slimb/β-TrCP. *Genes & Dev.* **13:** 284–294.

Taipale, J., Chen, J.K., Cooper, M.K., Wang, B., Mann, R.K., Milenkovic, L., Scott, M.P., and Beachy, P.A. 2000. Effects of oncogenic mutations in Smoothened and Patched can be reversed by cyclopamine. *Nature* **406:** 1005–1009.

von Mering, C. and Basler, K. 1999. Distinct and regulated activities of human Gli proteins in *Drosophila*. *Curr. Biol.* **9:** 1319–1322.

Wang, G., Wang, B., and Jiang, J. 1999. Protein kinase A antagonizes Hedgehog signaling by regulating both the activator and repressor forms of Cubitus interruptus. *Genes & Dev.* **13:** 2828–2837.

Wicking, C., Shanley, S., Smyth, I., Gillies, S., Negus, K., Graham, S., Suthers, G., Haites, N., Edwards, M., Wainwright, B., et al. 1997. Most germ-line mutations in the nevoid basal cell carcinoma syndrome lead to a premature termination of the PATCHED protein, and no genotype-phenotype correlations are evident. *Am. J. Hum. Genet.* **60:** 21–26.

Winston, J.T., Strack, P., Beer-Romero, P., Chu, C.Y., Elledge, S.J., and Harper, J.W. 1999. The SCFβ–TRCP–ubiquitin ligase complex associates specifically with phosphorylated destruction motifs in IκBα and β-catenin and stimulates IκBα ubiquitination in vitro. *Genes & Dev.* **13:** 270–283.

Yamasaki, L. and Pagano, M. 2004. Cell cycle, proteolysis and cancer. *Curr. Opin. Cell Biol.* **16:** 623–628.

Yoon, J.W., Liu, C.Z., Yang, J.T., Swart, R., Iannaccone, P., and Walterhouse, D. 1998. Gli activates transcription through a herpes simplex viral protein 16-like activation domain. *J. Biol. Chem.* **273:** 3496–3501.

Downloaded from on November 20, 2024 - Published by Cold Spring Harbor Laboratory Press

Dual degradation signals control Gli protein stability and tumor formation

Erik G. Huntzicker, Ivette S. Estay, Hanson Zhen, et al.

Genes Dev. 2006, **20:**
Access the most recent version at doi:10.1101/gad.1380906

Supplemental Material https://genesdev.cshlp.org/content/suppl/2006/01/18/gad.1380906.DC1

Related Content **Protein Degradation Regulates Sonic Hedgehog Signals**
Sci. STKE February , 2006 2006: tw51

References This article cites 34 articles, 17 of which can be accessed free at:
https://genesdev.cshlp.org/content/20/3/276.full.html#ref-list-1

Articles cited in:
http://genesdev.cshlp.org/content/20/3/276.full.html#related-urls

License

Email Alerting Service Receive free email alerts when new articles cite this article - sign up in the box at the top right corner of the article or **click here.**

Cold Spring Harbor Laboratory Press